ELSEVIER

Journal of Fluids and Structures 18 (2003) 715–728

JOURNAL OF FLUIDS AND STRUCTURES

www.elsevier.nl/locate/jnlabr/yjfls

# Lock-on characteristics of a cavity shear layer

C.-H. Kuo*, W.I. Jeng

*Department of Mechanical Engineering, National Chung-Hsing University, 250, Kuo Kuang Road, Taichung 402, Taiwan, ROC*

Received 8 November 2002; accepted 23 July 2003

**Abstract**

This investigation focuses on defining the lock-on regions of a cavity shear layer subject to local periodic excitations. A circular cylinder of small diameter ($d = 4$ mm), located very close to the upstream edge of cavity, is used to generate the local periodic excitations in the form of oscillatory rotation about its center with various angular amplitudes ($\Delta\theta$) and frequencies ($f_e$). All the experiments were conducted in a recirculating water channel at three different Reynolds numbers that are based on the momentum thickness at the upstream edge of cavity ($\mathrm{Re}_{\theta_0} = 152$, 216 and 278). The LDV system and the laser-sheet technique are employed to perform the quantitative velocity measurements and the qualitative flow visualization, respectively. For cavity flows at three Reynolds numbers studied, the resonant lock-on is found to be the primary lock-on region within the range of frequency ratio ($f_e/f_0 = 0.28-2.0$). Here $f_0$ denotes the natural instability frequency of an unexcited cavity shear layer. The frequency bandwidth of resonant lock-on region does increase with increasing excitation amplitudes ($\Delta\theta$). While the excitation amplitudes are smaller than 5° ($\Delta\theta \leqslant 5°$), the resonant lock-on region, at Reynolds numbers 216 and 278, distributes asymmetrically about $f_e/f_0 = 1.0$ and biases to the high frequency (or large $f_e/f_0$) side. However, the sidewise expansion of resonant lock-on region is enlarged and the degree of asymmetric distribution is alleviated at large excitation amplitudes ($\Delta\theta > 5°$). The amount of sidewise expansion of the resonant lock-on region biased toward the high-frequency side is more significant at the lowest Reynolds number (152) than those at two higher Reynolds numbers (216 and 278). Besides, there exists a sub-harmonic lock-on region only at the lowest Reynolds number 152. The existence of a sub-harmonic lock-on region clearly reveals that the differential equation governing the self-excited oscillation within a cavity contains the quadratic nonlinear term. Further, at the lowest Reynolds number (152), the sidewise expansion of the sub-harmonic lock-on region is much narrower than that of the resonant lock-on region.


## 1. Introduction

In the past decades, cavity flows in various engineering applications have received great attention due to their practical importance. For high-speed applications, the flows over the surface cut outs of aircraft may produce acute noise; serious buffeting (Heller and Bliss, 1975) and cause significant increase of the cavity drag (Gharib and Roshko, 1987). On the other hand, the vibration of a hydraulic gate slot and the heat transport efficiency over a powered electronic chip on a printed circuit board (Ghaddar et al., 1986) represent some important low-speed applications of cavity flows.

Flow separation takes place at the upstream edge of the cavity because of the geometric discontinuity, and a thin free shear layer forms thereafter. The separated thin shear layer becomes unstable and grows exponentially in the streamwise direction. Then, the unstable shear layer impinges on the downstream edge of cavity. Immediately after the impingement, a pressure fluctuation created near the impinging surface reflects toward the upstream edge of cavity at

*Corresponding author. Tel.: +886-422840433x419; fax: +886-422877170.
*E-mail address:* chkuo@dragon.nchu.edu.tw (C.-H. Kuo).

0889-9746/$ - see front matter © 2003 Elsevier Ltd. All rights reserved.
doi:10.1016/j.jfluidstructs.2003.08.020

**Nomenclature**

| | |
|---|---|
| $A$ | excitation amplitude |
| $D$ | cavity depth, 3.5 cm |
| $f_0$ | natural instability frequency of cavity shear layer |
| $f_e$ | excitation frequency |
| $L$ | cavity width, 7.0 cm |
| PSD | power spectral density |
| $\mathrm{Re}_{\theta_0}$ | Reynolds number based on momentum thickness at $x = 0$ (e.g., $U_0\theta_0/\nu$) |
| $S$ | spanwise dimension |
| $\mathrm{St}_{\theta_0}$ | Strouhal number based on momentum thickness at $x = 0$ (e.g., $f_0\theta_0/U_0$) |
| $\mathrm{St}_L$ | Strouhal number based on the cavity width, $f_0L/U_0$ |
| $U_c$ | convection speed of the unstable shear layer |
| $\bar{u}_{\min}$ | minimum velocities across the shear layer, measured at $x/L = 0.5$ |
| $\bar{u}_{\max}$ | maximum velocities across the shear layer, measured at $x/L = 0.5$ |
| $U_0$ | uniform inflow |
| $\bar{u}(L/2, y)$ | cross-flow profile of mean streamwise velocity, measured at $x = L/2$ |
| $\bar{u}(x, y)$ | mean streamwise velocity |
| $\tilde{u}$ | streamwise velocity fluctuation |
| $\partial\bar{u}/\partial y$ | velocity gradient across the shear layer |
| $x, y, z$ | the streamwise, transverse and spanwise coordinate system |
| $y^+$ | $y^+ = (y - y_{0.5})/\theta(x)$ |
| $U^*$ | $(\bar{u}(L/2, y) - \bar{u}_{\min})/(\bar{u}_{\max} - \bar{u}_{\min})$ |
| $y_{0.5}$ | the elevation where $U^* = 1/2$ |

*Greek letters*

| | |
|---|---|
| $\theta(x)$ | local momentum thickness along the shear layer |
| $\theta_0$ | momentum thickness at the upstream edge of the cavity |
| $\lambda$ | wavelength of the unstable shear layer |

the speed of sound, completing the feedback loop. As the flow reaches certain critical conditions, both the selective amplification characteristics of the cavity shear layer and the upstream propagating feedback provide necessary conditions for the oscillations within a cavity to be self-excited. This oscillation exhibits a sharp and strong spectral peak at a frequency corresponding to the shear layer instability (Rockwell and Naudascher, 1978; Gharib and Roshko, 1987). Thus, a large pressure fluctuation is sustained within the cavity and is responsible for the fatigue damage of the components around or inside a cavity (Ethembabaoglu, 1973).

In an attempt to understand the key mechanism and resolve these undesirable problems, the cavity-related investigations had been studied intensively during the past (Rockwell and Naudascher, 1978). Characteristics of the self-excited oscillation within a cavity depend upon several important factors. First of all, the flow conditions at the upstream edge play critical roles on the oscillating characteristics across a cavity. For instance, the magnitude of an incoming velocity, momentum thickness at the upstream edge and the width/depth ratio of a cavity (Knisely and Rockwell, 1982; Gharib, 1987; DeMetz and Farabee, 1977) determine the oscillating mode and the amplitude within the cavity. Second, the vertical offset at the downstream edge of a cavity also strongly affects the oscillating amplitude (Rockwell and Knisely, 1979). For example, as the downstream edge of the cavity is replaced by a ramp, the amplitude of fluctuating pressure inside the cavity and the aero-acoustic noise can be reduced effectively (Ethembabaoglu, 1973; Franke and Carr, 1975). Further, based upon the results of Kuo and Huang (2001), the bottom slope (either positive or negative) of a cavity can also change the oscillating characteristics of the cavity shear layer to different extents. And, the negative bottom slope is found to have better performance than the positive one to reduce the oscillating amplitude.

Besides, the oscillating amplitude can be greatly enlarged as the excitation frequency lies within the selective frequency range of the shear layer instability, provided that the excitation amplitude is larger than a threshold value (Gharib, 1987). Recently, an investigation on the self-excited oscillations within a cavity in the presence of a horizontal cover plate has been made in an application to the lower reservoir of a pumped-storage hydroelectric power plant (Huang, 1998 and Kuo et al., 2000). The presence of a horizontal cover plate in the vicinity of a cavity greatly enhances the oscillating amplitude of the unstable cavity shear layer. Furthermore, the leading-edge bluntness of a cover plate

also changes the oscillating mode and/or the oscillating amplitude within cavity (Kuo and Huang, 2000). In a hydroelectric power plant, the flow usually possesses certain frequency components imposed on the mean flow. So far, the effect of periodic excitations on the oscillating amplitude within a cavity (or gate slot) has received little attention, and the related phenomena still remain unknown. This motivates the present investigation on the lock-on characteristics of a cavity shear layer subject to periodic excitations. Practically, it is difficult to generate a quasi-two-dimensional pulsating flow in a test-section. Thus, a local excitation technique is applied at the most sensitive region of the cavity shear layer so as to study the response of an excited cavity shear layer. In this study, a simplified two-dimensional rectangular cavity model (or gate slot) is employed. A small circular cylinder, located very near the upstream edge of cavity (Fig. 1), generates an oscillatory rotation about its center at various angular amplitudes ($\Delta\theta$) and excitation frequencies ($f_e$). This local excitation serves as the only source of the periodic excitation.

This paper is organized in the following manner. Section 2 describes the geometry of the cavity model, the definition of the coordinate system, the flow conditions, the measurement techniques and related details of the data acquisition system. In Section 3, the mean and the dynamic characteristics of an unexcited cavity shear layer are illustrated first as a reference case. This is followed by the response characteristics of an excited shear layer and the comparison with those of an unexcited one. Subsequently, the results subject to various excitation amplitudes and at different Reynolds numbers are discussed. Finally, possible mechanisms responsible for these responses are outlined based on a nonlinear theory describing the self-excited oscillation subject to local periodic excitations. The objective is to reveal the lock-on characteristics of an excited cavity shear layer.

## 2. Experimental set-ups

### 2.1. Setups of cavity model and coordinate system

As shown in Fig. 1, the width/depth ratio of the two-dimensional rectangular cavity model is $L/D = 2$. The cavity model is located downstream of an accelerating ramp whose profile is machined precisely to a fifth-order polynomial by the CNC machine. The profile of this accelerating ramp is designed to maintain a uniform in-flow condition in the outer flow regime and an attached boundary-layer flow at the upstream edge of cavity. Further, the "surface polishing" process employs the slurry as a lubricant to obtain a lustrous surface. It is intended to minimize the influence of surface roughness on the boundary-layer structure, especially at the upstream edge of cavity. The ramp profile merges smoothly

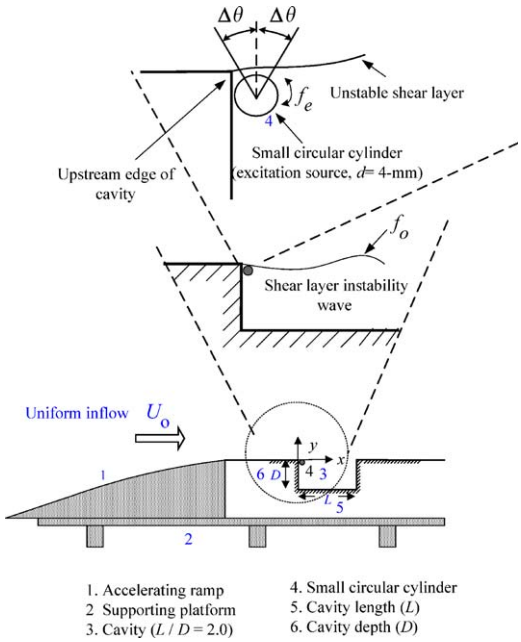


Fig. 1. Experimental set-up showing the coordinate system of cavity model, the enlarged view of small cylinder and some important parameters.

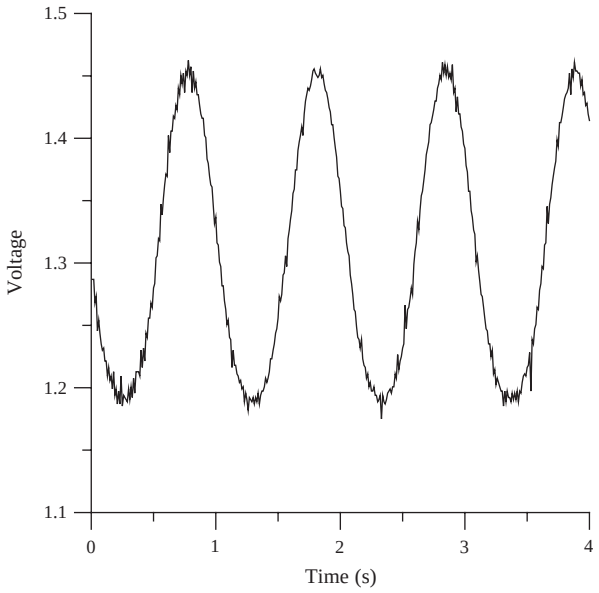


Fig. 2. Typical time signal of the rotary oscillation of the small cylinder.

into a horizontal part located immediately upstream of the cavity. The two-dimensional cavity model has an aspect ratio $S/D = 11.2$ and rests on a full-span two-dimensional horizontal platform placed 5 cm above the bottom of the test-section. The flow rate between the platform and the channel bottom is regulated carefully, so that the uniform in-flow has a zero incidence angle relative to the leading edge of the accelerating ramp.

As sketched in Fig. 1, the origin of the coordinate system is located at the upstream edge of cavity. The directions along and upward normal to the incoming flow define the positive $x$ and $y$ directions, respectively. And, $z = 0$ defines the plane at mid-span where the flow visualization and the extensive velocity measurements are performed. During flow visualization, fluorescent dye is fed by gravity through a constant but low-head reservoir. In such a design, the dye can be released naturally and steadily from a tiny hole of 0.5 mm diameter situated about $15\theta_0$ upstream of the origin (e.g., at $x = 0$ or at the upstream edge of cavity). The laser beam, from a continuous wave laser, passes a collimator and finally reaches the planar-cylindrical lens where the beam is converted into a laser sheet. The thickness of laser sheet is about 0.6–0.8 mm. Then, the self-excited oscillatory flow pattern can be illuminated and visualized by casting the laser light sheet on the plane at mid-span. A CCD camera, having 1/30 s shutter speed, is employed to continuously capture the images of the time-dependent flow pattern.

In the present study, a small circular cylinder has a 4 mm diameter and is employed to generate the local periodic excitations. The cylinder length is about 102% of the whole span and is rigidly supported on both sides of the supporting frame. The small cylinder is located very close to the upstream edge (or at $x/L = 0.03$ and $y/D = -0.06$) of the cavity to ensure the generation of a single-frequency excitation. The periodic excitations are in the form of oscillatory rotation about the center of the small cylinder. Mathematically, the motion of this rotating cylinder can be expressed as $\theta(t) = \Delta\theta \sin(2\pi f_e t)$. In the present study, the angular excitation amplitude $\Delta\theta$ is kept constant while the excitation frequency changes from $f_e/f_0 = 0.28$ to 2.0. In addition, different angular amplitudes ($\Delta\theta$) are selected to study the effect of excitation amplitude. Under this arrangement, the top surface of the small cylinder is tangent to the low-speed side of the cavity shear layer. The oscillatory rotation of the small cylinder is driven from one end by a servomotor, via which the excitation amplitudes and frequencies can be controlled precisely, with minimum attainable excitation amplitude around $\pm 0.36^\circ$. A typical trace of the periodic excitation, depicted in Fig. 2, clearly exhibits not only good periodicity but also stable amplitude from cycle to cycle, with negligible noise. Further, the lock-on and the non-lock-on regimes are identified at three different Reynolds numbers.

### 2.2. Experimental conditions

All experiments were performed in a recirculating water channel. The test-section has a cross-section of 40 cm × 40 cm and is 300 cm long. At the upstream edge (or $x = 0$), the mean streamwise velocity profiles $\bar{u}(x, y)$, measured at different spanwise locations, resemble the Blasius boundary-layer profile within 96.3% of the whole span, and have shape factors

around $2.56 \pm 0.21$. The maximum deviation of $\bar{u}(x, y)$ is about 1.62% from the Blasius solution. Near the upstream edge of the cavity (e.g., $x = 0$ mm, $y$=0.05 mm), a hydrogen-bubble wire is placed horizontally along the spanwise direction to qualitatively visualize the top-view flow structure across the cavity. The top-view flow structure is observed as a smooth surface across the cavity mouth up to $x/L = 0.8$ (namely, a quasi-two-dimensional laminar shear flow). Inside the cavity, a large-scale recirculation flow pattern represents the principal flow structure that remains quasi-two-dimensional in nature.

For all the experiments, the free water surface is maintained at 25 cm (or $307\theta_0$) above the cavity. Before and after installing the accelerating ramp with the cavity model into the test-section, all the velocity spectra, measured at various streamwise locations and across the height of test-section, show only wide-band characteristics at the noise level without any spectral peak. These preliminary tests further ensure no detectable oscillation induced by the free water surface at these Reynolds numbers.

In the present study, we examine the spanwise straightness of the small cylinder and the two-dimensional nature of the flow by several indirect methods. The straight small cylinder is made of Tungsten carbide that has high rigidity ($E = 630$ GPa) and high yield strength (2400 MPa). From simple beam theory, the maximum static deflection is predicted to be around 1.65 μm at mid-span due to its own weight. Theoretically, there will be no velocity fluctuation in the radial direction while the cylinder, rotating continuously in one direction in the quiescent fluid, is perfectly straight. On the other hand, any deflection of the rotating cylinder can induce periodic (or nearly periodic) velocity fluctuations in the radial direction in the near field because the deflected rotating cylinder whirls in a circular orbital path around the supporting axis. During the test, the velocity fluctuations in the radial direction are taken by the LDA system at the half-span section in the vicinity of rotating cylinder, while the small cylinder rotates continuously in one direction at the highest rate (3.0 Hz) in quiescent liquid. After several tests, no discernible spectral peak was found in the velocity spectra. This implies that there are no detectable periodic radial velocity fluctuations induced by the deflection of the small rotating cylinder. Further, the mean streamwise velocity profiles behind the rotating cylinder are also examined at several locations within 96.3% of the whole span. Similar velocity profiles are found with maximum deviation of 1.54% of $U_0$. These preliminary examinations further ensure that, by all experimental means we can attain, the small rotating cylinder is straight and the flow behind the rotating cylinder is two-dimensional in nature.

Concerning the natural frequency of the small cylinder, a cantilevered cylinder having the same material and the same diameter but only half the length was tested in quiescent fluid. The natural frequency of the small cylinder has found to be around 70 Hz, which is about 14.3% lower than the theoretical value at the same supporting condition. The viscous damping and the added mass effects in the quiescent fluid are the primary cause for this underestimated value. In theory, the natural frequency for the fixed–fixed support condition is about 1.7 times (around 138 Hz) that of the fixed–free supporting case for the same length. Thus, the natural frequency of the small cylinder in the present experiment is far away from the natural instability frequency ($f_0$) of the cavity shear layer and no contamination will be introduced on the response frequency of the excited shear layer.

### 2.3. Quantitative velocity measurements

For the experimental conditions studied herein, the preliminary tests mentioned in the previous section ensure the quasi-two-dimensional flow structure across the cavity. Therefore, velocity measurements performed by a laser Doppler velocimetry (LDV) system on the plane at mid-span (at $z = 0$) can truly reveal the typical unsteady flow structures across the cavity. The LDV system, operated in backscatter mode, consists of a continuous wave laser source, a Bragg cell for frequency shifting, and an integrated transmitting and receiving module. A correlation-based signal processor is employed to validate the data within each Doppler burst. It is the advantage of this nonintrusive technique that no probe interference is introduced during the measurements, especially within the most sensitive region of the cavity shear layer. A traversing table of 0.01 mm accuracy controls the measuring locations within the flow field. Furthermore, the small size of the seeding particles ($TiO_2$, 8 μm in averaged diameter) in water flow gives a responding time around 6.2 μs. Relative to the time scale in water flow, both the sufficiently fast response time (6.2 μs) and the small Stokes number (0.001) of the seeding particles ensure that the particle motion will follow the fluid motion naturally without slip. In addition, proper seeding concentration in the water gives continuous velocity time signals acquired by the LDV system.

Within the flow region, the validated data rate is around 1000–2000 $s^{-1}$. Before entering the data acquisition system, all the time signals of the validated velocity are fed into a low-pass filter having 100 kHz bandwidth to avoid aliasing. A 12-bit A/D converter whose maximum sampling rate is 330 kHz then digitizes the velocity signals. To obtain the mean velocity within the flow field, a sampling period including 80 s (or 80 cycles) indeed provides the statistically averaged value. The relative uncertainty of uniformity of the incoming velocity was estimated to be about $0.53\% U_0$. For the oscillatory flow measurements, the excitation frequency ratio ($f_e/f_0$) ranges between 0.28 and 2.0. The sampling frequency of 100 Hz and the sampling period of 40.96 s (or 40 cycles) give a frequency resolution of 0.024 Hz and

a cut-off frequency of 50 Hz. Furthermore, measurements of the velocity fluctuation $\tilde{u}$ are performed on the high-speed side of cavity shear layer where the local streamwise velocity reaches $90\%U_0$. Two different FFT algorithms are employed to calculate the power spectral density functions in this study. The first one is the decimation-in-time FFT algorithm in which the total number of sampled data is a power of 2. The second approach is the Turkey–Cooley algorithm that calculates the power spectral density function when the total number of the sampled data-point is any integer $N$. The spectra calculated by these two approaches, both with a Hanning window, give similar spectral density functions and thus the same lock-on and non-lock-on regions.

At each measuring location, an average of 10 sample PSD functions yields the ensemble-averaged PSD by which the lock-on and non-lock-on regions are defined. Since we only have finite (ten) measurements, the analysis of $t$-distribution can be used to quantify the difference between the finite mean and the population mean. Based on this method, the deviation between the finite mean and the population mean is calculated to be about $0.7\Delta f$, where $\Delta f$ is the frequency resolution of each estimated spectrum. Therefore, the responding frequency of each spectral peak can be correctly identified. For further validation of this error estimation, examinations of all ten power spectral densities show that all the responding frequencies indeed fall within the predicted range.

## 3. Results and discussion

### 3.1. Mean and dynamic characteristics of unexcited cavity shear layer

The streamwise velocity profiles $\bar{u}(L/2, y)$ are measured across the shear layer at $x/L = 0.5$ for different flow conditions. When the small cylinder is stationary ($f_e = 0$), the velocity profile $\bar{u}(L/2, y)$ across the cavity shear layer, measured at $x/L = 0.5$, serves as a reference case. In Fig. 3, the streamwise velocity profile across the cavity shear layer is nondimensionalized as $U^*$ and the ordinate is $y^+$. Definitions of the symbols $\bar{u}_{\max}$, $\bar{u}_{\min}$, $\theta(x)$ and $y_{0.5}$ are given in Nomenclature. The normalized velocity profiles $U^*$, measured at $x/L = 0.5$, are shown in Fig. 3 only for some representative cases. For the simple cavity without a small cylinder (triangular symbols), the normalized velocity profile $U^*$ distributes uniformly in the region far away from the cavity (e.g., $y^+ \gg 0$). Across $y^+ = 0$, there is a significant velocity gradient ($\partial\bar{u}/\partial y$), signifying the approximate location of the unstable cavity shear layer. Inside the cavity, the magnitude of $U^*$ reduces to zero due to very slow recirculation motion inside the cavity. When a stationary small cylinder is located very near the upstream edge of cavity (solid circle), the two velocity profiles evidently collapse onto a single curve. A similar $U^*$ distribution is also observed for the case of an oscillatory rotating cylinder at relatively large

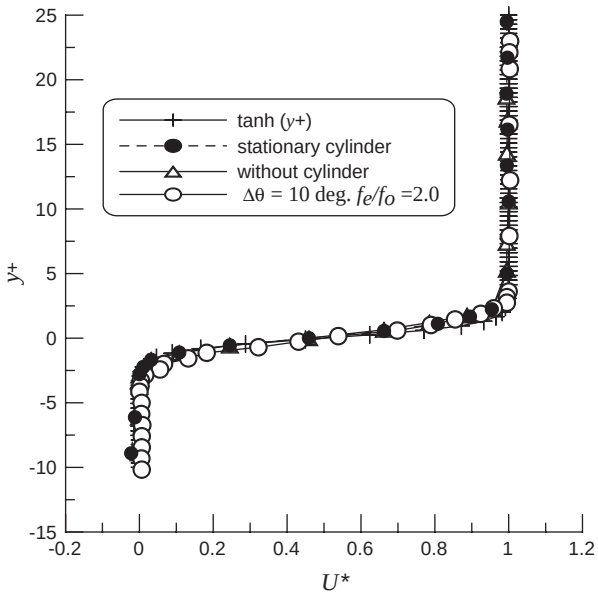


Fig. 3. Nondimensional cross-flow velocity profiles $U^*$ at different flow conditions. The velocity profiles are measured at $x/L = 0.5$.

amplitude and high excitation frequency (open circles). In Fig. 3, all the velocity distributions $U^*$ closely fit onto the theoretical tanh-velocity profile (solid line). This reveals that neither placing a stationary small cylinder nor an oscillatory cylinder will cause the mean velocity profiles $U^*$ to deviate away from the theoretical thin shear layer (tanh-velocity) profile.

Besides, snapshots of the unstable shear layer across the cavity are depicted in Figs. 4(a) and (b) for the cases of a simple cavity without and with a stationary small cylinder. Typical velocity spectra acquired from the velocity fluctuation $\tilde{u}$ near the shear layer are also shown in Figs. 4(c) and (d). Both the power spectral density functions peak well above the noise level, clearly indicating the existence of self-excited oscillation within the cavity. In both cases, the responding peak frequencies are very close to each other ($f_0 = 1.12$ Hz) and their corresponding Strouhal numbers $\mathrm{St}_{\theta_0}$, based on these peak frequencies, equal 0.0168. These values are very close to the theoretical value (0.017) based upon the velocity profile of thin shear layer (Blake, 1980). On the other hand, the wavelengths of both unstable shear layers are estimated about $\lambda/L = 0.58$ from flow visualization [Figs. 4(a) and (b)]. By rearranging the parameter $\mathrm{St}_L$ as the ratio $(L/\lambda)(U_c/U_0)$, the wavelengths for both cases are calculated around $\lambda/L = 0.60$ based on the measured convection velocity ($U_c \approx 0.52U_0$).

According to the foregoing results of wavelength and responding frequency in both cases, it is clear that installation of a small circular cylinder very near the upstream edge of cavity neither influences the instability nature of the unstable shear layer nor does the mean velocity profile $U^*$. Namely, the instability characteristics of cavity shear layers, either unexcited or excited, can still be predicted by linear stability theory based on the tanh velocity profile of thin shear layers.

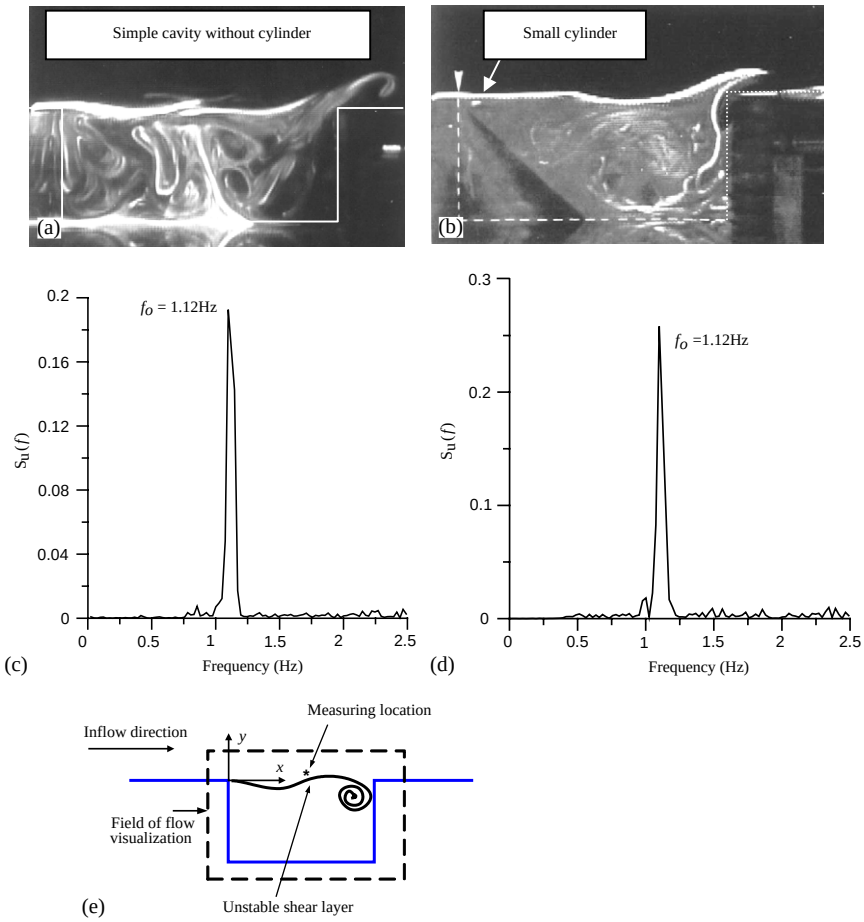


Fig. 4. (a, c) Snapshot and power spectral density $S_u(f)$ of the natural mode of self-excited oscillation within a simple cavity without cylinder; (b, d) with small stationary cylinder. Here $f_0$ represents the natural frequency of self-excited oscillation within a cavity. Note that, the wavelengths of the unstable shear layer in (a and b) approximately equals, $\lambda = 0.58L$.

### 3.2. Response characteristics of an excited shear layer

As defined in the literature (Hall and Griffin, 1993), the flow characteristic is categorized as "non-lock-on" when only the natural frequency component ($f_0$) of shear layer instability becomes dominant. On the other hand, the "lock-on" characteristic is defined as long as the spectral component, centered at the excitation frequency ($f_e$), becomes dominant and completely replaces the natural component ($f_0$) of shear layer instability. In-between the adjacent lock-on and non-lock-on regions, the velocity spectra exhibit two spectral peaks of comparable magnitude. Their corresponding peak frequencies are equal to the excitation frequency ($f_e$) and the natural instability frequency ($f_0$) of the unstable shear layer, respectively. This kind of flow is defined as the "boundary region". The boundary region signals the transition of an excited shear layer between the natural mode (or non-lock-on mode) and the lock-on mode of oscillation within the cavity.

When the cavity shear layer is perturbed at the smallest excitation amplitude ($\Delta\theta = \pm 2^\circ$), the power spectral density $S_u(f)$ measured at $x/L = 0.6$ on the high-speed side of the shear layer are illustrated in Fig. 5 in a sequence of increasing frequency ratio ($f_e/f_0 = 0.28-2.0$); $f_0$ represents the natural mode of shear layer instability within a cavity, and $f_e$ denotes the excitation component. The Reynolds number is 152 in this case.

As the frequency ratio ranges between 0.28 and 0.4, there exist several spectral peaks at frequencies $f_e$, $2f_e$ and $f_0$ in the power spectral density $S_u(f)$ of Fig. 5, indicating the boundary characteristics of the excited cavity shear layer. At $f_e/f_0 = 0.50$, the sharp spectral peak at $f_e$ overwhelms the natural component at $f_0$. This corresponds to the lock-on characteristic of an excited shear layer, responding at one half of the natural instability frequency ($f_0$) of the cavity shear layer. Thus, this lock-on feature is termed as the "sub-harmonic lock-on" region hereafter.

The lock-on feature is replaced by boundary characteristics when the frequency ratio becomes $f_e/f_0 = 0.55$. However, starting from $f_e/f_0 = 0.6$ and up to $f_e/f_0 = 1.41$, the spectral peak of excitation component ($f_e$) completely dominates within the cavity. This feature denotes another lock-on band of the excited cavity shear layer. Since this frequency band

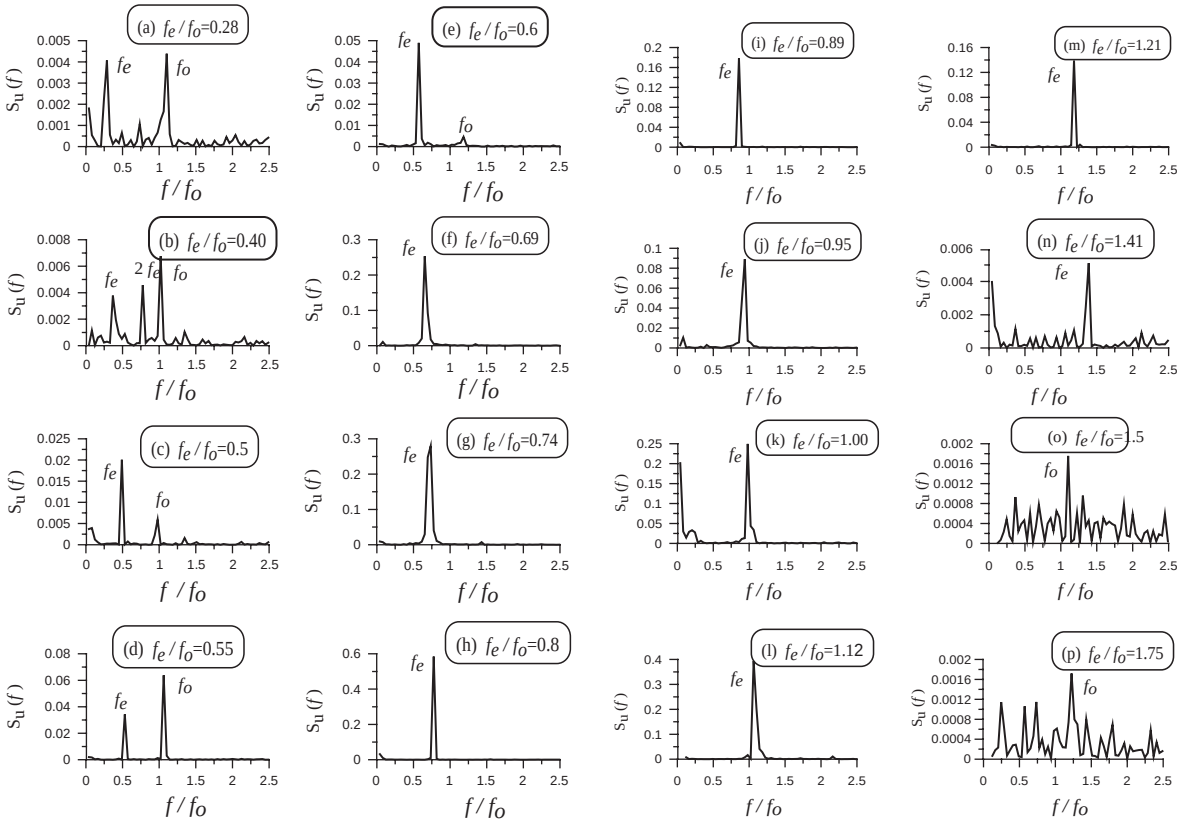


Fig. 5. Power spectral density $S_u(f)$ of the velocity fluctuation $\tilde{u}$, measured on the high-speed side of cavity shear layer, for various excitation frequencies ratio ($f_e/f_0$). Note that the oscillating amplitude is $\Delta\theta = \pm 2^\circ$. The units for $S_u(f)$ are ($cm^2/s$). The Reynolds number, based on the momentum thickness $\theta_0$, equals 152.

is centered at the nature frequency of shear layer instability, it is referred as the "resonant lock-on" region hereafter. Beyond the frequency ratio $f_e/f_0 = 1.50$, the spectral peak at the excitation frequency ($f_e$) diminishes abruptly. In this case, the spectral peak of the natural component of shear layer instability becomes dominant. The power spectral density $S_u(f)$ of this kind is categorized as a characteristic of the "non-lock-on" regions.

### 3.3. Effect of excitation amplitudes on lock-on bands

Four different excitation amplitudes ($\Delta\theta = 2^\circ$, $5^\circ$, $8^\circ$, $10^\circ$) of periodic excitations are selected to define the boundaries of the lock-on regions, while the frequency ratio ranges from $f_e/f_0 = 0.28$ to 2.0. When the excitation amplitude equals $\Delta\theta = \pm 5^\circ$, the power spectral density function of velocity fluctuations, measured at $x/L = 0.6$, are shown in Fig. 6 in a sequence of increasing frequency ratio.

When the excitation frequency ratio lies between 0.28 and 0.4 in Fig. 6, several spectral peaks are present in the power spectral density functions. Here the natural component of shear layer instability ($f_0$) is largely dominant. This clearly corresponds to the non-lock-on characteristics of the cavity shear layer. On the contrary, at $f_e/f_0 = 0.5$, the sharp spectral peak centered at $f_e$ becomes dominant again, indicating the existence of a sub-harmonic lock-on region. As the frequency ratio increases slightly to $f_e/f_0 = 0.55$, two spectral peaks of comparable magnitude are observed in the power spectral density function $S_u(f)$. This feature clearly illustrates the boundary characteristic between two adjacent lock-on regions.

As the frequency ratio reaches $f_e/f_0 = 0.6$, a very sharp spectral peak reappears at the excitation frequency, and no other spectral peaks are found. The power spectral density of this kind clearly reveals the lock-on characteristic at this excitation frequency. When the frequency ratio lies between $f_e/f_0 = 0.6$ and 1.50, the dominance of spectral peak still

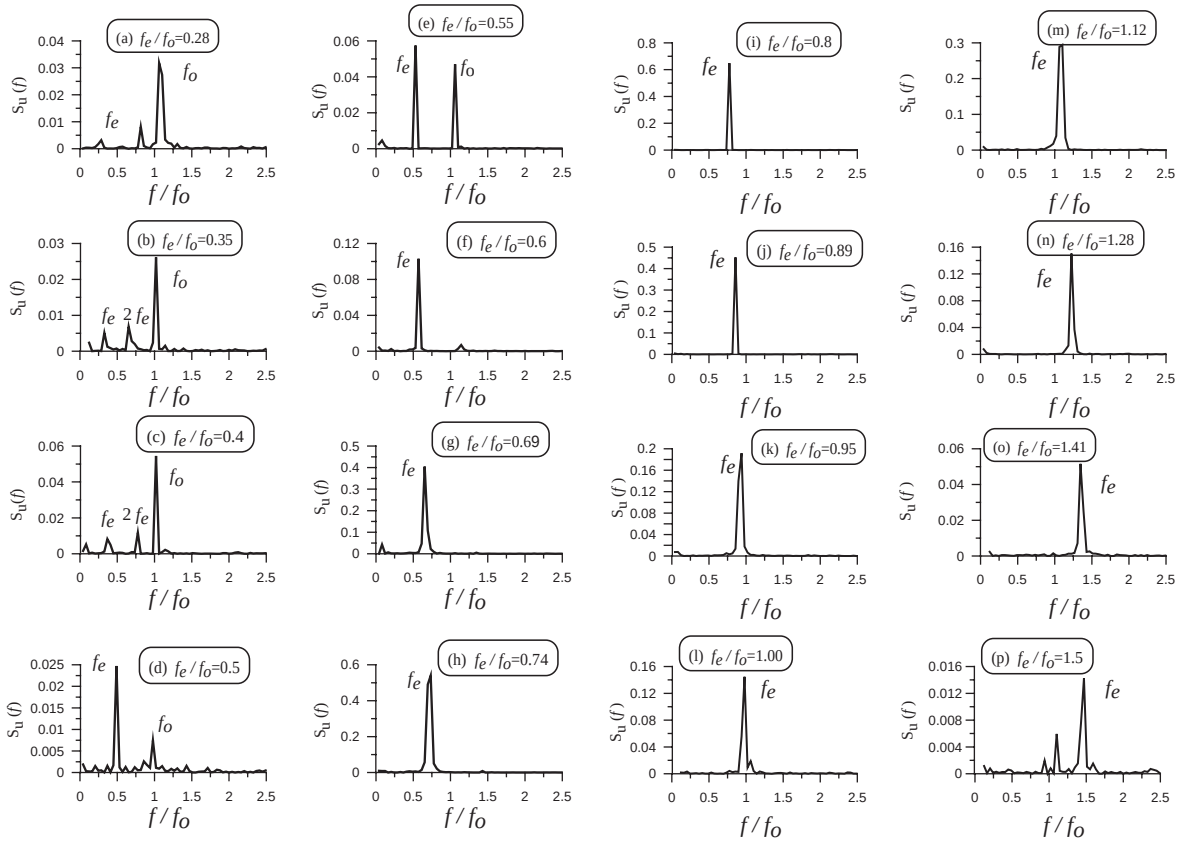


Fig. 6. Power spectral density $S_u(f)$ of the velocity fluctuation $\tilde{u}$, measured on the high-speed side of cavity shear layer, for various excitation frequencies ratio ($f_e/f_0$). Note that the oscillating amplitude is $\Delta\theta = \pm 5^\circ$. The units for $S_u(f)$ are ($cm^2/s$). The Reynolds number, based on the momentum thickness $\theta_0$, equals 152.

appears at the excitation frequency ($f_e$), indicating a lock-on region. This response characteristic corresponds to the resonant lock-on region.

When the Reynolds number equals 152, the lock-on regions of an excited shear layer within cavity are summarized in Fig. 7 as functions of excitation amplitudes and excitation frequencies. It is clear that two lock-on regions are found within the frequency range $f_e/f_0 = 0.28$–$2.0$ for $\Delta\theta \leqslant \pm 5^\circ$. One lock-on region is centered at the sub-harmonic frequency ($f_0/2$), and the other is centered at the fundamental frequency ($f_0$) of shear layer instability in the cavity. A boundary region separates the sub-harmonic and the resonant lock-on regions. The bandwidth of sub-harmonic lock-on region is much narrower than that of the resonant lock-on region. It is also found that the resonant lock-on region expands significantly toward the high-frequency side as the excitation amplitude enlarges. When the excitation amplitudes exceed $\Delta\theta = \pm 8^\circ$, the sub-harmonic and the resonant lock-on regions merge into each other, leading to only one single lock-on region within the same frequency range ($f_e/f_0 = 0.28-2.0$).

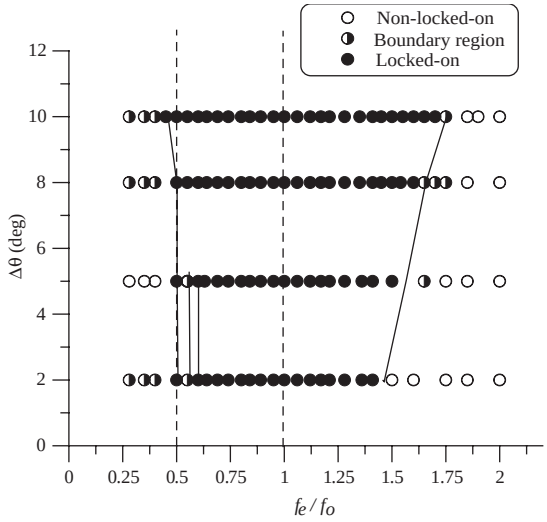


Fig. 7. Map of the lock-on, non-lock-on and boundary regions of an excited cavity shear layer as functions of excitation amplitudes and frequencies; the Reynolds number, based on the momentum thickness $\theta_0$, equals 152.

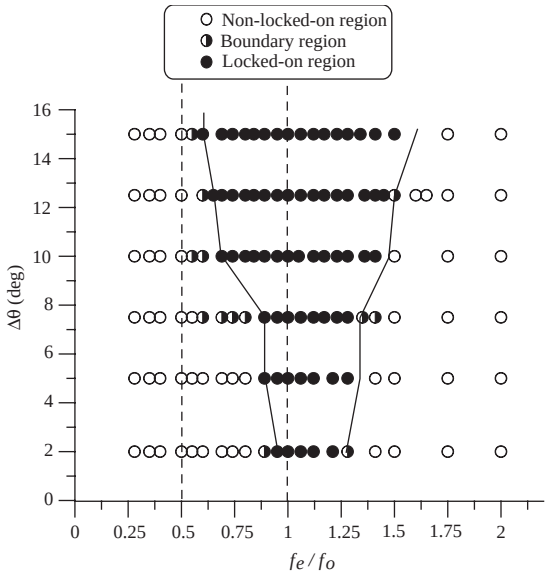


Fig. 8. Map of the lock-on, non-lock-on and boundary regions of an excited cavity shear layer as functions of excitation amplitudes and frequencies; the Reynolds number, based on the momentum thickness $\theta_0$, equals 216.

### 3.4. Effect of Reynolds number on lock-on bands

Fig. 8 depicts the map defining the lock-on, boundary and non-lock-on regions at a higher Reynolds number (216). It is clear that within the same range of frequency ratio ($f_e/f_0 = 0.28-2.0$), the sub-harmonic lock-on region disappears at this Reynolds number. Moreover, there is only one single lock-on region, known as the resonant lock-on region. The frequency bandwidth of resonant lock-on region is much narrower than that in Fig. 7. Likewise, the frequency bandwidth of resonant lock-on region depends strongly upon the excitation amplitudes. Namely, the bandwidth of the resonant lock-on region broadens with increasing excitation amplitudes. A remarkable finding is that the resonant lock-on band distributes asymmetrically about the frequency ratio $f_e/f_0 = 1.0$ while the excitation amplitude is small. Namely, it expands more significantly toward the high-frequency side than to the low frequency direction. As the excitation amplitude increases beyond $\Delta\theta = \pm 10^\circ$, the degree of asymmetric distribution about $f_e/f_0 = 1.0$ gradually diminishes.

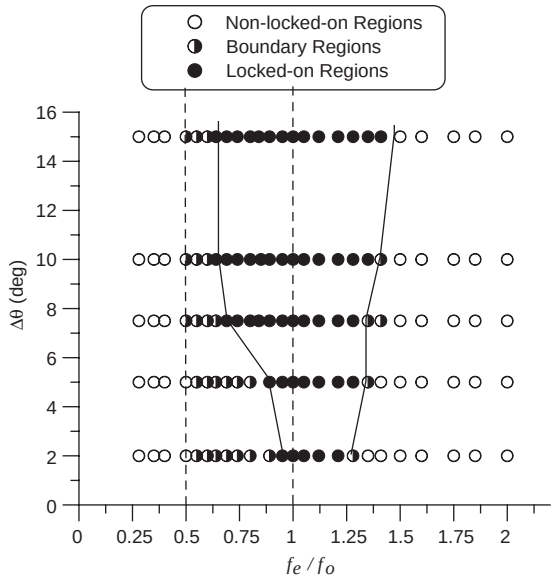


Fig. 9. Map of the lock-on, non-lock-on and boundary regions of an excited cavity shear layer as functions of excitation amplitudes and frequencies; the Reynolds number, based on the momentum thickness $\theta_0$, equals 278.

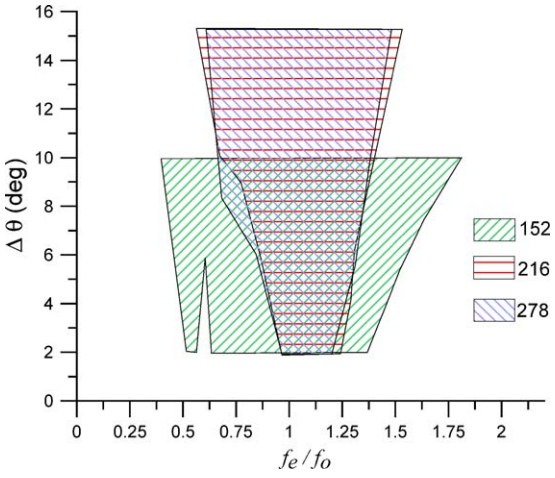


Fig. 10. Direct comparison of the resonant lock-on regions of an excited cavity shear layer at three different Reynolds numbers.

When the Reynolds number increases further up to 278, the lock-on regions are defined in Fig. 9 as functions of excitation frequencies and excitation amplitudes. Similarly to the results shown in Fig. 8, the sub-harmonic lock-on region is missing within the same range of excitation frequency ratio ($f_e/f_0 = 0.28-2.0$). The bandwidths of resonant lock-on region are about the same as that of Fig. 8 at small excitation amplitudes. However, the bandwidths of the lock-on region shrink slightly at large excitation amplitudes. Likewise, the asymmetric distribution of resonant lock-on region is reduced when the excitation amplitudes ($\Delta\theta$) are greater than $8^\circ$. To examine the Reynolds number effect, the lock-on regions for three different Reynolds numbers are plotted in Fig. 10 for direct comparison. It is clear that the resonant lock-on region is broadest at the lowest Reynolds number (152) for which the self-excited oscillation within cavity is at the onset stage. The sub-harmonic lock-on region exists only at the lowest Reynolds number. The resonant lock-on region displays a significantly reduced broadness when the Reynolds number increases from 152 to 216. However, the frequency bandwidth of the resonant lock-on region does not change significantly for two higher Reynolds numbers (216 and 278).

### 3.5. Possible mechanism that affects lock-on region and bandwidth

In the case of no external excitation, the unstable cavity shear layer exhibits a self-excited oscillation at the natural instability frequency ($f_0$). The characteristics of self-excited oscillation within cavity can be described by nonlinear ordinary differential equations with quadratic and/or cubic nonlinear terms (Nayfeh and Mook, 1979). In the case of the lowest Reynolds number (152), the existence of a sub-harmonic lock-on region clearly reveals that the differential equation governing the self-excited oscillation in the cavity flows contains the quadratic nonlinear term.

When the excitation frequency ($f_e$) lies in the neighborhood of the natural instability frequency ($f_0$) of cavity shear layer, the excited shear layer will respond at the excitation frequency. This flow characteristic clearly belongs to the resonant lock-on category. Further, the sidewise expansion of resonant lock-on region depends strongly upon the excitation amplitudes (Nayfeh and Mook, 1979). Namely, the larger the excitation amplitudes are, the wider the resonant lock-on band. Also, from theory, the resonant lock-on region will distribute symmetrically about $f_e/f_0 = 1.0$ when the excitation energy remains constant.

For the cases of nonresonant excitations, the excitation frequencies ($f_e$) are far away from the natural frequency ($f_0$), and the sub-harmonic and super-harmonic frequencies $f_0/n$ and $nf_0$, where $n$ is any positive integer. In this case, the external excitation may change the system characteristics appreciably from a positive damping to a negative value if the excitation amplitude exceeds a certain threshold value. This change is primarily caused by the nonlinear interaction between the excitation component ($f_e$) and the natural instability component ($f_0$) of the cavity shear layer. In case of a positive damping, the excitation component is damped out. Thus, only the natural component of the shear layer instability exists and dominates the flow field. This flow characteristic is associated with a non-lock-on feature. Further increase of the excitation amplitude beyond a threshold value will change the system damping to a negative value and cause the natural instability component ($f_0$) of the cavity shear layer to decay completely. This phenomenon is called "quenching". In this case, the responding frequency is the same as that of the excitation frequency, and the flow characteristic is associated with a lock-on feature.

In the present study, the existence of a resonant lock-on region is caused by the primary resonance when the excitation frequency lies in the neighborhood of $f_e/f_0 = 1.0$. For all the Reynolds numbers studied herein, the resonant lock-on regions show different amounts of sidewise expansion, depending upon the excitation amplitudes (Figs. 7–9). However, in the resonant lock-on region, where the excitation amplitudes are large and the excitation frequencies are far away from the natural instability frequency of the cavity shear layer, the quenching phenomenon may play an important role and is primarily responsible for extra sidewise expansion of the resonant lock-on region.

At the Reynolds numbers 216 and 278, the asymmetric distribution of the resonant lock-on region is more significant at small excitation amplitudes ($\Delta\theta \leqslant 5^\circ$) than that at large ones ($\Delta\theta > 5^\circ$). The reason for this asymmetric distribution is discussed in what follows. In the present study, the angular displacement ($\Delta\theta$) of periodic excitation is kept constant while the excitation frequency ($f_e$) changes. Given an angular amplitude ($\Delta\theta$), the excitation amplitude of the tangential velocity generated by a small rotating cylinder equals $2\pi fe\Delta\theta$ and is linearly proportional to the excitation frequency. Even at small excitation amplitudes ($\Delta\theta \leqslant 5^\circ$), the tangential velocity excitations will be large at high excitation frequencies. Thus, the asymmetric distribution of resonant lock-on region, depicted in Figs. 7–8, toward the high-frequency end is primarily due to the unequal tangential velocity excitations on either side of $f_e/f_0 = 1.0$. However, at large excitation amplitudes ($\Delta\theta > 5^\circ$), the quenching mechanism provides an additional opportunity for the excited shear layer to be locked-on by the external excitations at low excitation frequencies. Thus, the degree of asymmetric distribution of the resonant lock-on region is diminished at large excitation amplitudes. In other words, at large excitation amplitudes, the primary resonance and/or the quenching phenomenon are the two main mechanisms that

cause significant sidewise expansion on either side of the resonant lock-on region, and thus reduce the degree of asymmetric distribution about $f_e/f_0 = 1.0$.

For the lowest Reynolds number (152), the sidewise expansion is mild at all excitation amplitudes employed, and the distribution of resonant lock-on region is only slightly asymmetric about $f_e/f_0 = 1.0$. At this Reynolds number, the self-excited oscillation is at its onset stage and the oscillating amplitude of the unstable shear layer at a frequency $f_0$ is relatively small. Thus, applications of the same excitation amplitude can easily induce the primary resonance and the quenching mechanism leading to the lock-on flow characteristics. Therefore, at the lowest Reynolds number, the sudden sidewise expansion of resonant lock-on region is more pronounced and the asymmetric distribution toward the high frequency is diminished.

In a nonlinear oscillatory system, the onset of a sub-harmonic lock-on region is caused by the nonlinear interaction between the excitation component ($f_e$) and the natural instability component ($f_0$) of the cavity shear layer. At the lowest Reynolds number, the oscillating amplitude of the unstable shear layer is small relative to that of the external excitation. Applications of the same excitation amplitudes can easily induce the quenching mechanism leading to a sub-harmonic lock-on flow characteristic. Thus, the sub-harmonic lock-on region exists only at the lowest Reynolds number.

Existence of a sub-harmonic lock-on region and very narrow sidewise expansion of the sub-harmonic lock-on region clearly reveal that the differential equation governing the self-excited oscillation in the cavity flows contains a weak quadratic nonlinear term.

## 4. Concluding remarks

Lock-on characteristics of an excited cavity shear layer are studied experimentally in a recirculating water channel. The LDV system and the laser sheet technique are employed to perform the quantitative velocity measurements and the qualitative flow visualization, respectively. The local periodic excitations are generated by a small circular cylinder, located very near the upstream edge of cavity, in the form of an oscillatory rotation about its center with various angular amplitudes ($\Delta\theta$) and frequencies ($f_e$). Under such experimental conditions, the lock-on regions of an excited cavity shear layer are defined. Also, the Reynolds number effect is investigated.

For all the Reynolds numbers employed herein, the resonant lock-on characteristic of an excited cavity shear layer is found to be the primary lock-on region within the frequency range $f_e/f_0 = 0.28$–$2.0$. Within the same frequency range, the frequency bandwidth of the resonant lock-on region indeed increases significantly with increasing excitation amplitudes for Reynolds numbers 216 and 278, but changes mildly at Reynolds number 152.

The resonant lock-on region is caused by the primary resonance if the excitation frequency ($f_e$) lies in the neighborhood of $f_e/f_0 = 1$. When the excitation amplitudes are large enough and the excitation frequencies ($f_e$) are far away from the natural instability frequency ($f_0$) of the cavity shear layer, the "quenching" phenomenon may provide another important mechanism to cause sudden sidewise expansion of the resonant lock-on region.

For Reynolds numbers 216 and 278 and at small excitation amplitudes ($\Delta\theta \leqslant 5^\circ$), the resonant lock-on region distributes asymmetrically about $f_e/f_0 = 1.0$ and is biased toward the high-frequency side. The unequal excitation amplitude of tangential velocity about $f_e/f_0 = 1.0$ is primarily responsible for the asymmetric distribution of the resonant lock-on region toward the high-frequency direction. At large excitation amplitudes ($\Delta\theta > 5^\circ$), the sidewise expansion of the resonant lock-on region is enlarged and the degree of asymmetric distribution is reduced because both the primary resonance and the quenching mechanisms make contributions.

At the lowest Reynolds number, the oscillating amplitude of the unexcited cavity shear layer is relative small. Thus, the external excitation at the same amplitude can easily induce both the primary resonance and the quenching mechanism, leading to the lock-on flow characteristics. Therefore, the sidewise expansion of resonant lock-on region toward the high-frequency side is more significant at the lowest Reynolds number than at higher ones.

In a nonlinear oscillatory system, the onset of a sub-harmonic lock-on region is caused by the nonlinear interaction between the excitation component and the natural component of cavity shear layer (Nayfeh and Mook, 1979). At the lowest Reynolds number (152), the existence of a sub-harmonic lock-on region and a very narrow sidewise expansion clearly reveal that the differential equation governing the self-excited oscillation within the cavity flows contains weak quadratic nonlinear term.

## Acknowledgements

The authors are grateful for the project supported by the National Science Foundation of the Republic of China under the Grant No. NSC-87-2212-E-005-026.

## References

Blake, W.K., 1980. . Mechanics of Flow-Induced Sound and Vibration. Vol. 1: General Concept and Elementary Sources. Academic Press, London (Chapter 3).

DeMetz, F.C., Farabee, T.M., 1977. Laminar and turbulent shear flow induced cavity resonance. AIAA Paper No. 77-1293.

Ethembabaoglu, S., 1973. On the fluctuating flow characteristics in the vicinity of gate slots. Ph.D. Dissertation, Division of Hydraulic Engineering, Norwegian Institute of Technology, University of Trondhelm.

Franke, M.E., Carr, D.L., 1975. Effect of geometry on open cavity flow-induced pressure oscillations. AIAA Paper No. 75-492.

Ghaddar, N.K., Korczak, K.Z., Mikic, B.B., Patera, A.T., 1986. Numerical investigation of incompressible flow in grooved channels—stability and self-sustained oscillation. Journal of Fluid Mechanics 163, 99–127.

Gharib, M., 1987. Response of the cavity shear layer oscillations to external forcing. AIAA Journal 25 (1), 43–47.

Gharib, M., Roshko, A., 1987. The effect of flow oscillations on cavity drag. Journal of Fluid Mechanics 177, 501–530.

Hall, M.S., Griffin, O.M., 1993. Vortex shedding and lock-on in a perturbed flow. ASME Journal of Fluids Engineering 115, 283–291.

Heller, H.H., Bliss, D., 1975. The physical mechanism of flow-induced pressure fluctuations in cavities and concepts for their suppression. AIAA Paper No. 75-491.

Huang, S.H., 1998. Experimental study and control on oscillatory characteristics of cavity shear layer. Master Thesis, Department of Mechanical Engineering, National Chung Hsing University, Taichung, Taiwan, ROC.

Knisely, C., Rockwell, D., 1982. Self-sustained low frequency components in an impinging shear layer. Journal of Fluid Mechanics 116, 157–186.

Kuo, C.H., Huang, S.H., 2000. Influence on cavity shear flows by horizontal cover-plate with different leading-edge profiles, Proceedings of the Seventh International Conference on Flow Induced Vibrations, Lucerne, Switzerland, pp. 167–172.

Kuo, C.H., Huang, S.H., 2001. Influence of flow path modification on oscillation of cavity shear layer. Experiments in Fluids 31, 162–179.

Kuo, C.H., Huang, S.H., Chang, C.W., 2000. Self-sustained oscillation induced by horizontal cover plate above the cavity. Journal of Fluids and Structures 14 (1), 25–48.

Nayfeh, A.H., Mook, D.T., 1979. Nonlinear Oscillations. Wiley, New York.

Rockwell, D., Naudascher, E., 1978. Review of self-sustaining oscillations of flow past cavities. Transaction of ASME, Journal of Fluids Engineering 100, 152–165.

Rockwell, D., Knisely, C., 1979. The organized nature of flow impingement upon a corner. Journal of Fluid Mechanics 93 (3), 413–432.